Volume 1 | Number 1 | Jan 2013 | Pages 1–100

Dalton Transactions

An international journal of inorganic chemistry
www.rsc.org/dalton

ROYAL SOCIETY OF CHEMISTRY

ROYAL SOCIETY OF CHEMISTRY

www.rsc.org/dalton

Journal Name

ARTICLE

Novel Open-Framework Europium Silicates Prepared under High-Temperature and High-Pressure Conditions

Wei Liu,[a] Ying Ji,[a] Xinjian Bao,[a] Ying Wang,[a] Benxian Li,[b] Xiaofeng Wang,[a] Xudong Zhao,*[a] Xiaoyang Liu*[a,b] and Shouhua Feng[a]

Two new europium silicates, $Na_{15}Eu_3Si_{12}O_{36}$ (denoted as **1**) and $K_2EuSi_4O_{10}F$ (denoted as **2**), were successfully synthesized under high-temperature and high-pressure conditions, and structurally characterized by single-crystal and powder X-ray diffraction (XRD). The single-crystal XRD analysis of **1** reveals that its structure is based on $[Si_6O_{18}]_n^{12n-}$ cyclosilicate anions that are built from six SiO_4 tetrahedra sharing two of their four O corners with each other. Such $[Si_6O_{18}]_n^{12n-}$ cyclosilicate anions are linked via EuO_6 octahedra to form a three-dimensional (3D) framework containing 6-membered ring channels delimited by the SiO_4 tetrahedra and EuO_6 octahedra along the [010] direction. The structure of **2** consists of infinite tubular chains of corner-sharing SiO_4 tetrahedra, which are further linked together via corner sharing O atoms by infinite chains of EuO_4F_2 octahedra forming a 3-D framework that contains 8-ring and 6-ring channels along the [010] direction. The photoluminescence properties of **1** and **2** were also investigated.

Introduction

Recently, many studies have focused on the synthesis of microporous silicates of transition metals,[1-9] main group elements,[10-13] lanthanides,[14-20] and uranium[21-24] because of their versatile structural chemistry as well as interesting physical and chemical properties. Among them, lanthanide silicates, which contain stoichiometric amounts of framework Ln^{3+} ions, have high thermal stability and tunable optical properties, making them potential candidates as fast ion conductors and optical materials. In 1997, Rocha et al. first reported the synthesis of a microporous sodium yttrium silicate $Na_4K_2Y_2Si_{16}O_{38} \cdot 10H_2O$ (AV-1) under mild hydrothermal conditions at 503 K in Teflon-lined autoclaves.[25] Since then, a series of lanthanide silicates AV-n (n = 2, 5, 9, 20, 23)[14,18,26-28] have been successfully prepared under mild hydrothermal conditions. Their structures and tunable luminescent properties derived from the multiple Ln^{3+} ions have also been investigated. Recently, Wang et al. reported a new luminescent microporous terbium silicate containing helical sechser (six) silicate chains and 9-ring channels.[19] Other lanthanide silicates with the same structure were also reported by Ananias et al.[29]

In recent decades, high-temperature and high-pressure synthetic method have attracted considerable attention for the synthesis of microporous lanthanide silicates and germanates that cannot be obtained under mild hydrothermal conditions. In 1993, Haile et al. successfully prepared a number of

neodymium and yttrium silicates under high-temperature and high-pressure hydrothermal conditions.[30,31] In 2005, Lii et al. reported a new europium silicate, $Cs_3EuSi_6O_{15}$, which contains only tertiary $[SiO_4]$ tetrahedra.[32] This is the second example of a 3-D silicate framework with a Si/O ratio of 2:5. High-temperature and high-pressure synthetic method is widely used in the synthesis of microporous transition metals, and uranium silicates as well.[3,6,21,22] With continuous interest in the exploratory synthesis of lanthanide silicates and germanates under high-temperature and high-pressure conditions, our group has reported a number of rare earth element (REE) disilicates, and microporous lanthanide silicates/germanates with special structures.[32-36] For instance, in 2012, we reported three new lanthanide silicates based on anionic silicate chains, layers, and framework prepared under high-temperature and high-pressure conditions.[33] In this work, we report two new europium silicates, $Na_{15}Eu_3Si_{12}O_{36}$ and $K_2EuSi_4O_{10}F$, which were synthesized under high-temperature and high-pressure conditions, and their structures and photoluminescence properties were also investigated.

Experimental

Synthesis of Na$_{15}$Eu$_3$Si$_{12}$O$_{36}$

Single crystals of the title compound (Compound **1**) were synthesized from the reaction mixture of 0.12 g NaOH (Beijing Chemical Factory, 99.9%), 0.0522 g Eu$_2$O$_3$ (Aldrich, 99.9%), and 0.1083 g SiO$_2$ (Aldrich, 99.9%) (molar ratio Na/Eu/Si=10:1:6), in a piston-cylinder-type apparatus at 500 MPa, 400 °C for 48 h. Pressure was calibrated from melting of dry NaCl at 1050 °C[37] and the transformation of quartz to coesite at 500 °C.[38] The experimental temperature was monitored by a Pt100%–Pt90%Rh10% thermocouple inserted into the high-pressure cell. The starting mixture was encapsulated in a sealed platinum tube with a diameter of 5mm and a height of 8 mm, which was separated by MgO powder from a graphite heater. The reaction was quenched before the pressure was released. The resulting colourless crystals were washed with distilled water and dried in air at 60 °C.

Synthesis of K$_2$EuSi$_4$O$_{10}$F

The title compound (Compound **2**) was synthesized from a KF·2H$_2$O-KOH flux. The synthesis was carried out under autogenous pressure in a silver tube contained in a hydrothermal research system (Model HR-1B-2, LECO Tem-Pres), where pressure was provided by water. Typically, a mixture of 0.62 g KF·2H$_2$O (Beijing Chemical Factory, 99.9%), 0.07 g KOH (Beijing Chemical Factory, 99.9%), 0.105 g Eu$_2$O$_3$ (Aldrich, 99.9%), and 0.1430 g SiO$_2$ (Aldrich, 99.9%) (molar ratio K/Eu/Si = 12.8: 1: 4) was placed in a 5 cm silver tube (inside diameter = 4.90 mm), heated to 600 °C and maintained at this temperature for 48 h. The pressure was estimated to be 220 MPa according to the pressure-temperature diagram of pure water. After the reaction, the autoclave was slowly cooled to 300 °C followed by the removal of the autoclave from the furnace to cool the mixture rapidly to room temperature. The resulting colorless crystals were filtered, washed with deionized water, and dried at 60 °C.

Characterizations

Powder X-ray diffraction (XRD) data were collected using a Rigaku D/Max 2550 V/PC X-ray diffractometer with graphite-monochromated Cu Kα radiation (λ = 0.15418 nm) at 50 kV and 200mA at room temperature. Energy-dispersive spectroscopy (EDS) analysis was carried out using an EDS system with a window attached to a JEOL JSM-6700F scanning electron microscope. The photoluminescence (PL) spectra were obtained on a FlouroMax-4 spectrophotometer with Xe 900 (150 W xenon arc lamp) as the light source. To eliminate the second-order emission from the source radiation, a cut-off filter was used during the measurement. All spectra were recorded at room temperature.

Single-crystal Structural Analysis

Suitable single crystals of **1**, and **2** with dimensions of 0.12 × 0.09 × 0.05 mm^3 and 0.16 × 0.07 × 0.05 mm^3, respectively, were selected for single-crystal XRD analysis. Intensity data were collected at a temperature of 296 K on a Bruker SMART APEX 2 micro-focused diffractometer using graphite-monochromated Mo Kα radiation (λ = 0.71073 nm) at 50kV and 0.6 mA. Data processing was accomplished with the APEX 2 processing program. Empirical absorption corrections based on symmetry equivalents were applied. The structures were solved by direct methods and refined by full-matrix least-squares techniques with the SHELXTL crystallographic software package. All heaviest atoms, Eu, Na, and Si for **1**, K, Eu, and Si for **2**, were unambiguously located in the Fourier maps, and then O atoms and F atoms were found in the

Table 1 Crystal Data and Structure Refinement for **1** and **2**

	Na$_{15}$Eu$_3$Si$_{12}$O$_{36}$	K$_2$EuSi$_4$O$_{10}$F
Empirical formula	Na$_{15}$Eu$_3$Si$_{12}$O$_{36}$	K$_2$EuSi$_4$O$_{10}$F
Formula weight	1713.81	521.52
Temperature	293(2) K	293(2) K
Wavelength	0.71073 A	0.71073 A
Crystal system, space group	Orthorhombic , *Pnnm*	Monoclinic , *P2$_1$/m*
Unit cell dimensions	a = 10.7143(9) Å α = 90°	a = 11.6796(8) Å α = 90°
	b = 7.5271(7) Å β = 90°	b = 8.5399(6) Å β =112.72°
	c = 10.4913(9) Å γ = 90°	c = 11.7874(8) Å γ =90°
Volume	846.10(13) Å^3	1084.47(13) Å^3
Z	1	4
Crystal size	0.12 × 0.09 × 0.05 mm	0.16 × 0.07 × 0.05 mm
Theta range for data collection	2.72 - 25.02 °	1.87 - 25.14
Limiting indices	-12 ≤ h ≤ 12, -8 ≤ k ≤ 8, -7 ≤ l ≤ 12	-13 ≤ h ≤ 11, -9 ≤ k ≤ 10, -14 ≤ l ≤ 13
Reflections collected / unique	4014 / 791 [R(int) = 0.0192]	5638/2074[R(int)=0.0191]
Completeness to theta = 25.02	100.0 %	99.5 %
Refinement method	Full-matrix least-squares on F^2	Full-matrix least-squares on F^2
Data / restraints / parameters	791 / 0 / 87	2074 / 0 / 178
Goodness-of-fit on F^2	1.004	1.065
Final R indices [I>2sigma(I)]	R$_1$ = 0.0288, wR$_2$ = 0.1068	R$_1$= 0.0282, wR$_2$ = 0.0794
R indices (all data)	R$_1$ = 0.0309, wR$_2$ = 0.1094	R$_1$ =0.0299, wR$_2$ = 0.0804
Largest diff. peak and hole	0.707 and -0.490 e.Å^{-3}	0.980 and -0.938 e. Å^{-3}
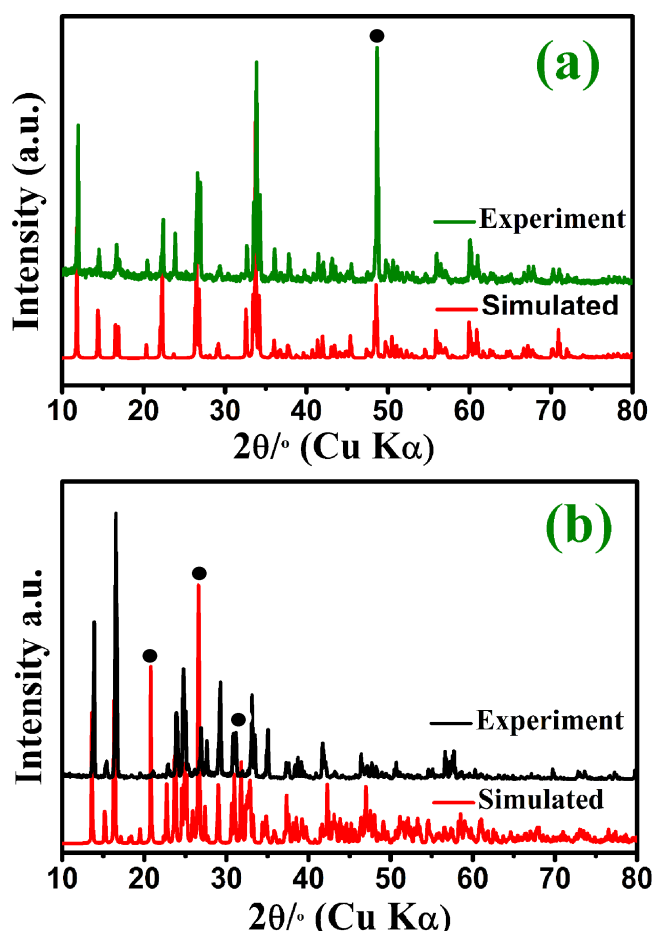
Figure 1 (a) Simulated and experimental powder XRD patterns of 1. (b) Simulated and experimental powder XRD patterns of 2. Black circles show the intensity difference of some reflections in the experimental XRD patterns from those observed in the simulated pattern caused by preferential orientation.

Figure 2 (a) Polyhedral view of the open-framework structure of **1** along the [110] direction. (b) The $[Si_6O_{18}]_n^{12n-}$ cyclosilicate anionic layer with 6- and 8-membered rings perpendicular to the [1-10] direction in **1**. (Color code: Eu, purple; Si, yellow. and bright green; Na, green; Na/Eu, orange).

subsequent difference Fourier maps. For **1**, single-crystal X-ray analysis showed that the crystallographic positions of Na(2) and Na(3) were also shared with partially occupied Eu(2) and Eu(3) atoms, respectively. The refined occupancies obtained for the Na and Eu refinements were 0.08/0.42 for the Eu(2)/Na(2) site and 0.045/0.205 for the Eu(3)/Na(3) site. EDS analysis results for select single crystals from the batch products of **1** and **2** were consistent with empirical formula given by single-crystal analyses (Figure S1 and table S1). The final cycles of least-squares refinement including atomic coordinates and anisotropic thermal parameters for all atoms converged at R_1=0.0288, wR_2=0.1068, and S=1.004 for **1**; R_1=0.0282, wR_2=0.0804, and S=1.065 for **2**; A summary of the crystallographic data is presented in Table 1. The selected bond lengths [Å] and angles [deg] for **1** and **2** are presented in Table S2 and Table S3 (Supporting Information). Atomic coordinates and equivalent isotropic displacement parameters for **1** and **2** are presented in Table S4 and Table S5.

Results and discussion

The powder XRD patterns of **1** and **2**, as shown in Figure 1, are consistent with the simulated XRD patterns based on the single-crystal structural analyses of **1** and **2**, indicating that they are isostructural. The intensity difference of some reflections in the experimental XRD patterns from those observed in the simulated pattern might result from preferential orientation (Black circles in Figure 1). Table S1 in the Supporting Information displays the EDS analysis results of the two compounds, which are in agreement with the theoretically calculated values given by single-crystal analyses.

Single-Crystal Structure of 1

Single-crystal structural analysis reveals that **1** crystallizes in the *Pnnm* space group (No.58) with *a* = 10.7143(9) Å, *b* = 7.5271(7) Å, and *c* = 10.4913(9) Å. Each asymmetric unit (Figure S2) of **1** contains one distinct Eu site, two symmetrically independent Si sites, and four distinct Na sites.
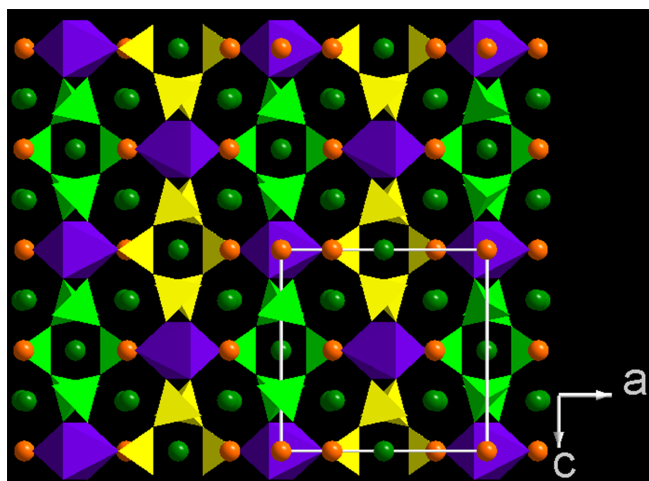
Figure 3 Polyhedral view of the open-framework structure of **1** along the [010] direction. (Color code: Eu, purple; Si, yellow and bright green; Na,green; Na/Eu, orange).

The Eu atom is coordinated to six bridging O atoms with the adjacent Si atoms to form a quite regular EuO_6 octahedron. The Eu–O bond lengths are between 2.295(4) Å and 2.307(5) Å, while the O–Eu–O angles vary from 81.5(2)° to 180.0(1)°.All of the Si sites are in 4-fold coordination to O atoms in tetrahedral geometry. The Si–O bond lengths are in the range of 1.562(4) – 1.637(4) Å and the O – Si – O angles in the range of 105.3(3)° – 117.2(2)°, which are within the normal range for silicates.

The SiO_4 tetrahedra share two of their four O corners with a corner of neighboring SiO_4 group to form 6-membered single rings with the composition $[Si_6O_{18}]^{12-}$. Such single $[Si_6O_{18}]^{12-}$ cyclosilicate anions, which are arranged in the [110] and [1-10] directions, respectively, result in $[Si_6O_{12}]_n^{12n-}$ cyclosilicate anions layers perpendicular to the [110] direction (Figure 2a). Figure 2b shows the 6-and 8-ring channels of $[Si_6O_{12}]_n^{12n-}$ cyclosilicate anions layers along the [110] and [1-10] directions. The 6-membered ring channels are delimited by six SiO_4 tetrahedra that belong to one $[Si_6O_{18}]^{12-}$ cyclosilicate anion, while the 8-membered ring channels are formed by eight SiO_4 tetrahedra that belong to four different $[Si_6O_{18}]^{12-}$ cyclosilicate anions. The $[Si_6O_{12}]^{12-}$ cyclosilicate anions and EuO_6 octahedra are connected via vertex oxygen atoms to form a three-dimensional framework of **1** (Figure 3). It contains 6-ring channels delimited by four SiO_4 tetrahedra and two EuO_6 octahedra along the [010] direction. The Na^+ ions are located in the free void space to achieve the charge balance. $Na(1)^+$ and $Na(4)^+$ ions are located in the 4- and 6-rings channels along the [010] direction, while $Na(2)^+$ and $Na(3)^+$ ions in the 6- and 8-rings channels along the [110] direction.

Single crystal X-ray analysis also reveals that the crystallographic positions of Na(2) and Na(3) are shared with partially occupied Eu(2) and Eu(3) centers, respectively. However, this statistical disorder is not unprecedented among the member of this structural family because of size similarity between the cationic radii of Ln^{3+} and Na^+.[39-41] To the best of our knowledge, Compound **1** is the first europium silicate with such a structure. Furthermore, this is the first attempt to

synthesize microporous lanthanide silicates under pressure higher than 300 MPa.

Single-Crystal Structure of 2

Compound **2** crystallizes in the $P2_1/m$ space group (No. 11) with a = 11.6796(8) Å, b = 8.5399(6) Å, c = 11.7874(8) Å, β = 112.72 °, and Z = 4. The asymmetric unit (Figure S3) of **2** contains one crystallographically distinct Eu site, four symmetrically independent Si sites, and four distinct K sites. All of the Si atoms are in 4-fold coordination to O atoms in a tetrahedral geometry. The observed Si – O bond lengths vary between 1.564(5) Å and 1.647(5) Å, while the O–Si–O bond angles range from 102.7(2)° to 114.1(3)°, which are within the normal range for silicates. Eu atom is six coordinated to four O atoms and two F atoms to form a relatively regular EuO_4F_2 octahedron. O^{2-} and F^- have the same number of electrons and therefor it is difficult to distinguish them clearly by single-crystal X-ray diffraction analysis. We consult the published literature about fluorosilicate and find that when oxygen and fluorine atoms are present in the structure, silicon atoms tend to bond with oxygen atoms to form highly stable SiO_4 tetrahedra. This phenomenon is common in fluorosilicates, such as $Eu_5F(SiO_4)_3$[42] and $K_5Eu_2FSi_4O_{13}$[43]. Therefor, we identify the axial atoms of each EuO_4F_2 octahedron, which act as common vertices to other EuO_4F_2 octahedra, are F atoms, while the other four equatorial atoms that connect with Si atoms are O atoms. According to the maximum cation-anion distance criterion by Donnay and Allmann, a limit of 3.35 Å is set for K–O interactions. Therefore, the coordination numbers of K atoms are as follows: K(1), 10-coordinate, including one F atom at 2.921(7)Å; K(2), 6-coordinate; K(3), 5-coordinate, including one F atom at 2.823(7) Å; and K(4), 7-coordinate, including one F atom at 2.763(7) Å.

As shown in Figure 4, the EuO_4F_2 octahedra and SiO_4 tetrahedra are linked by sharing vertex O atoms to form a 3-D framework of **2**. It contains a 6-membered ring and 8-membered channels that are delimited by tubular chains of corner-sharing SiO_4 tetrahedra and 1-D chains of EuO_4F_2 octahedra along the [010] direction (Figure 4a). The tubular chains of SiO_4 tetrahedra in the structures of 2 can be viewed as constructed from infinite number of 8-membered rings stacked in the sequence of [ABAB...] (Fig. 4b). Every EuO_4F_2 octahedron has four equatorial O atoms that are shared by three neighboring tubular silicate chains and two axial F atoms. These axial F atoms, act as common vertices to other octahedra forming a one-dimensional EuO_4F_2 octahedra chain along the [010] direction (Figure 4b). K(2) is located in the 8-ring channels delimited by eight SiO_4 tetrahedra, whereas the other K atoms are located in the 6-ring channels formed by four SiO_4 tetrahedra from two tubular chains and two EuO_4F_2 octahedra.It is worth mentioning that **2** is the first synthetic fluoride-silicate which contains tubular silicate chains and EuO_4F_2 octahedra chains in the structure.
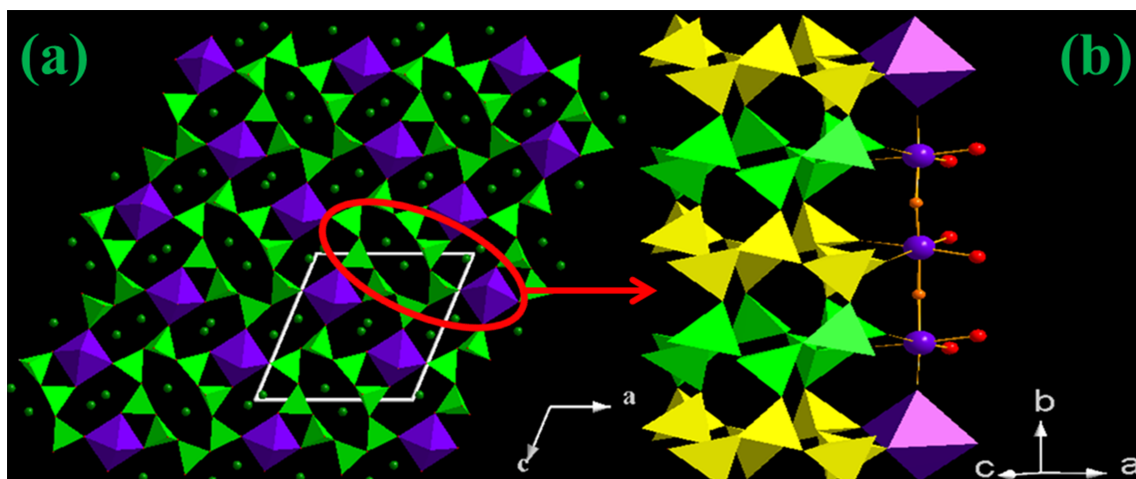
Figure 4 (a) Polyhedral view of the open-framework structure of **2** along the [110] direction. (b) Tubular chains constructed from infinite number of eight membered rings and EuO$_4$F$_2$ octahedra chains along the [010] direction. (Color code: Eu, purple; Si, yellow. and bright green; Na, green; F, orang
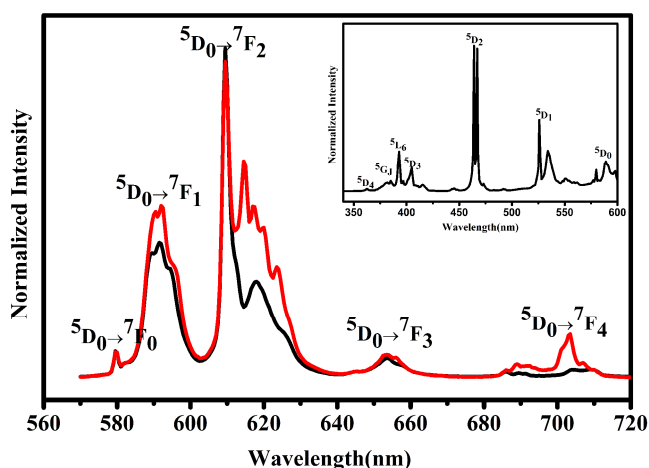
Figure 5 RT emission spectra of **1** (λ$_{em}$ = 395 nm, black line; λ$_{em}$ = 532 nm, red line). The inset shows the excitation spectrum of **1**, (λem = 610 nm)
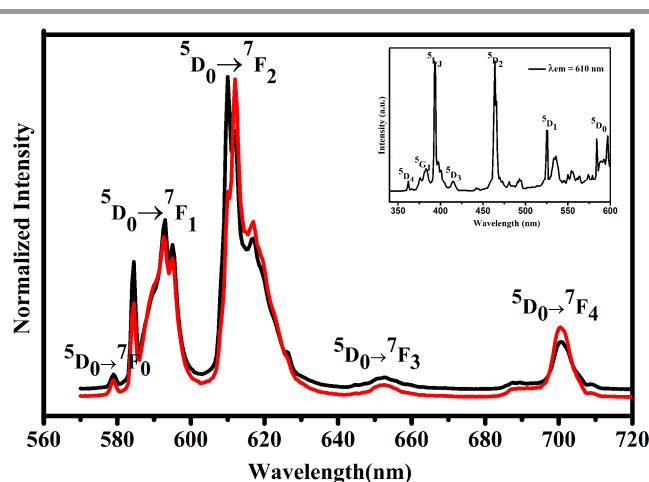
Figure 6 RT emission spectra of **2** (λex = 395 nm, black line; λex = 532 nm, red line). The inset shows the excitation spectrum of **2** (λem = 610 nm)

Photoluminescent studies

Figure 5 shows the room-temperature (RT) excitation and emission spectra of **1**. The excitation spectrum, monitored at the $^5D_0 \rightarrow {}^7F_2$ transition of Eu^{3+}, 610 nm, displays a series of sharp lines between 350 and 600 nm assigned to $^7F_{0-1} \rightarrow {}^5D_{4-0}$, $^5L_6$, and ^5G_J transitions of Eu^{3+}. The RT emission spectra of **1**, excited at 395 and 532 nm, show sharp emission lines from 560 to 720 nm, which can be ascribed to emission from the first excited $^5D_0$ state to $^7F_{0-4}$ Stark levels of fundamental Eu^{3+} septet. Luminescence from higher excited states, such as $^5D_1$, is not detected, indicating very efficient nonradiative relaxation to the $^5D_0$ level.

As shown in Figure 5, the $^5D_0 \rightarrow {}^7F_1$ and $^5D_0 \rightarrow {}^7F_2$ transitions are split into three and five Stark components by ligand field, indicating the presence of two or more Eu^{3+} environments. With the change of the excitation from 532 nm

($^5L_6$) to 395 nm ($^5D_2$), a decrease in the relative intensity of the $^5D_0 \rightarrow {}^7F_2$ transition and an increase in the relative intensity of the $^5D_0 \rightarrow {}^7F_1$ transition are observed. The observed changes in the relative intensity of the Eu^{3+} emission lines also indicate the existence of two or more local Eu^{3+} environments in **1**.[44,45] The $^5D_0 \rightarrow {}^7F_0$ transition acquires its intensity via an electric-dipole transition mechanism because of the lack of an inversion symmetry center of Eu^{3+}. According to the structural analysis, there are three crystallographically different Eu^{3+} ions in the structure, but only one $^5D_0 \rightarrow {}^7F_0$ transition was observed, which is due to the highly distorted pseudo-octahedral coordination environments of Eu(2)$^{3+}$ and Eu(3)$^{3+}$ ions. The Eu(1)$^{3+}$ ion is on a centrosymmetric site, furthermore, the Eu(1)O$_6$ octahedron is quite regular with the Eu – O bond lengths in the range of 2.295(4) Å to 2.307(5) Å. Therefore, the $^5D_0 \rightarrow {}^7F_0$ transition of Eu(1)$^{3+}$ could be too weak to be observed.[46,47] The intensity of the $^5D_0 \rightarrow {}^7F_2$ electric-dipole transition of Eu^{3+} is considerably stronger than that of the $^5D_0 \rightarrow$

$^7F_1$ magnetic-dipole transition. This indicates that there is a lack of an inversion-symmetry center on Eu^{3+} ions[48-50] which is consistent with the asymmetric Eu^{3+} location according to structural analysis. The $Eu(2)O_6$ octahedron and $Eu(3)O_6$ dodecahedron lack inversion symmetry and is strongly distorted because they are partially occupied $Na(2)$ and $Na(3)$ centers, respectively.

Figure 6 shows the RT excitation and emission spectra of **2**. The excitation spectrum, monitored at the $^5D_0 \rightarrow {}^7F_2$ transition of Eu^{3+}, 610 nm, displays a series of sharp lines between 350 and 600 nm attributed to $^7F_{0-1} \rightarrow {}^5D_{4-0}$, $^5L_6$, and ^5G_J transitions of Eu^{3+}. The RT emission spectra, excited at 394 and 532 nm, display a series of sharp lines from 560 to 720 nm, which are assigned to the $^5D_0 \rightarrow {}^7F_{0-4}$ transitions of Eu^{3+}. Luminescence from higher excited states is not detected, indicating very efficient nonradiative relaxation to the $^5D_0$ level. Different from the RT emission spectrum of **1**, the observed emission spectrum excited at 532 nm ($^5L_6$) is the same as that at the excitation of 395 nm ($^5D_2$). Furthermore, only one sharp line is present in the region for $^5D_0 \rightarrow {}^7F_0$ transition. This indicates the presence of one Eu^{3+} local environment. If the Eu^{3+} site lacks a center of symmetry, the intensity of the allowed $^5D_0 \rightarrow {}^7F_2$ electric-dipole transition is stronger than that of the allowed $^5D_0 \rightarrow {}^7F_1$ magnetic-dipole transition due to the ligand field effects. This result is consistent with the crystallographic result that EuO_4F_2 octahedron is quite regular and there is a lack of an inversion-symmetry center on Eu^{3+} ions.

Conclusions

Two new europium silicates with novel 3D novel frameworks, **1** and **2**, have been synthesized by using a high temperature and high pressure synthetic method. The structure of **1** is based on $[Si_6O_{18}]_n^{12n-}$ cyclosilicate anions that are linked via EuO_6 octahedra to form a 3D framework containing 6-membered ring channels along the [010] direction. The structure of **2** is constructed by infinite tubular silicate chains further connected by infinite chains of EuO_4F_2 octahedra resulting in a 3D framework structure that contains 8-ring and 6-ring channels along the [010] direction. The photoluminescence studies are consistent with the crystallographic results and show that both **1** and **2** exhibit strong red emissions. Compound **1** was obtained in a piston-cylinder-type apparatus at 500 MPa. To the best of our knowledge, this is the first attempt to synthesize microporous lanthanide silicates under pressure higher than 300 MPa. The successful syntheses of these two new europium silicates under high-temperature and high-pressure conditions will promote further research on lanthanide silicates with novel structures and special properties.

Acknowledgements

Notes and references

a State Key Laboratory of Inorganic Synthesis and Preparative Chemistry, College of Chemistry, Jilin University, 2699 Qianjin Street, Changchun, 130012, P. R. China; E-mail: liuxy@jlu.edu.cn ;

b College of Earth Sciences, Jilin University, 2199 Jianshe Street, Changchun, 130061, P. R. China

1   P. Brandão, A. Valente, A. Philippou, A. Ferreira, M. W. Anderson and J. Rocha, *Eur. J. Inorg. Chem*, 2003, **2003**, 1175.

2   R. J. Francis and A. J. Jacobson, *Angew. Chem. Int. Ed*, 2001, **40**.

3   L. I. Hung, S. L. Wang, H. M. Kao and K. H. Lii, *Inorg. Chem*, 2003, **42**, 4057.

4   L. I. Hung, S. L. Wang, S. P. Szu, C. Y. Hsieh, H. M. Kao and K. H. Lii, *Chem. Mater*, 2004, **16**, 1660.

5   C. Y. Li, C. Y. Hsieh, H. M. Lin, H. M. Kao and K. H. Lii, *Inorg. Chem*, 2002, **41**, 4206.

6   F. R. Loa and K. H. Lii, *J. Solid. State. Chem*, 2005, **178**, 1017.

7   M. Nyman, F. Bonhomme, D. M. Teter, R. S. Maxwell, B. X. Gu, L. M. Wang, R. C. Ewing and T. M. Nenoff, *Chem. Mater*, 2000, **12**, 3449.

8   R. D. Shannon, B. E. Taylor, T. E. Gier, H. Y. Chen and T. Berzins, *Inorg. Chem*, 1978, **17**, 958.

9   X. Wang, L. Liu and A. J. Jacobson, *Angew. Chem., Int. Ed*, 2001, **40**, 2174.

10   A. Ferreira, Z. Lin, J. Rocha, C. M. Morais, M. Lopes and C. Fernandez, *Inorg. Chem*, 2001, **40**, 3330.

11   A. Ferreiraa, Z. Linb, M. R. Soaresc and J. Rochab, *Inorg. Chim. Acta*, 2003, **356**, 19.

12   L. I. Hung, S. L. Wang, C. Y. Chen, B. C. Chang and K. H. Lii, *Inorg. Chem*, 2005, **44**, 2992.

13   L. I. Hung, S. L. Wang, S. P. Szu, C. Y. Hsieh, H. M. Kao and K. H. Lii, *Chem. Mater*, 2004, **16**, 1660.

14   D. Ananias, M. Kostova, F. A. A. Paz, A. Ferreira, L. D. Carlos, J. Klinowski and J. Rocha, *J. Am. Chem. Soc*, 2004, **126**, 10410.

15   D. Ananias, M. Kostova, F. A. A. Paz, A. N. C. Neto, R. T. D. Moura, O. L. Malta, L. D. Carlos and J. Rocha, *J. Am. Chem. Soc*, 2009, **131**, 8620.

16   P. Brandãoa, M. S. Reisb, Z. Gaic and A. M. d. Santos, *J Solid State Chem.*, 2013, **198**, 39.

17   M. H. Kostova, D. Ananias, F. A. A. Paz, A. Ferreira, J. Rocha and L. D. Carlos, *J. Phys. Chem. B*, 2007, **111**, 3576.

18   M. H. Kostovaa, D. Ananiasa, L. D. Carlosc and J. Rocha, *J. Alloys Compd*, 2008, **451**, 624.

19   G. Wang, J. Li, J. Yu, P. Chen, Q. Pan, H. Song and R. Xu, *Chem. Mater*, 2006, **18**, 5637.

20   G. Wang, W. Yan, P. Chen, X. Wang, K. Qian, T. Su and J. Yu, *Microporous. Mesoporous. Mater*, 2007, **105**, 58.

21   C. S. Chen, R. K. Chiang, H. M. Kao and K. H. Lii, *Inorg. Chem*, 2005, 44, 3914.

22   C. S. Chen, H. M. Kao and K. H. Lii, *Inorg. Chem*, 2005, 44, 935.

23   C. S. Chen, S. F. Lee and K. H. Lii, *J. Am. Chem. Soc*, 2005, **127**, 12208.

24   J. Huang, X. Wang and A. J. Jacobson, *J. Mater. Chem*, 2003, **13**, 191.

25 J. Rocha, P. Ferreira and Z. Lin, *Chem. Commun*,1997, 2103.

26 D. Ananias, A. Ferreira, J. Rocha, P. Ferreira, J. P. Rainho, C. Morais and L. D. Carlos, *J. Am. Chem. Soc*, 2001, **123**, 5735.

27 A. Ferreira, D. Ananias, L. D. Carlos, C. M. Morais and J. Rocha, *J. Am. Chem. Soc*, 2003, **125**, 14573.

28 J. Rocha, P. Ferreira, Z. Lin, P. Brandão, A. Ferreira and J. D. P. d. Jesus, *J. Phys. Chem. B*, 1998, **102**, 4739.

29 D. Ananias, F. A. A. Paz, L. D. Carlos and J. Rocha, *Microporous. Mesoporous. Mater*, 2013, **166**, 50.

30 S. M. Haile, B. J. Wuensch, T. Siegrist and R. A. Laudise, *J. Cryst. Growth*, 1993, **131**.

31 M. Y. Huang, Y. H. Chen, B. C. Chang and K. H. Lii, *Chem. Mater*, 2005, **17**, 5743.

32 X. Zhao, J. Li, P. Chen, Y. Li, Q. Chu, X. Liu, J. Yu and R. Xu, *Inorg. Chem*, 2010, **49**, 9833.

33 C. Wang, X. Liu, M. E. Fleet, S. Fenga and R. Xua, *J. Solid State Chem*, 2006, **179**, 2245.

34 C. Wang, X. Liu, M. E. Fleet, J. Li, S. Feng, R. Xu and Z. Jin, *Cryst Eng Comm*, 2010, **12**, 1617.

35 M. E. Fleet and X. Liu, *Am Mineral*, 2004, **89**, 396.

36 W. Liu, M. yang, Y. Ji, F. Y. Liu, Y. Wang, X. F. Wang, X. D. Zhao and X. Y. Liu, *RSC Adv*, 2014, **4**, 26951.

37 S. R. Bohlen, *Neues Jb. Mineral. Mh*, 1984.

38 S. R. Bohlen and A. L. Boettcher, *J. Geophys. Res*, 1982.

39 A. Ferreira, D. Ananias, L. D. Carlos, C. M. Morais and J. Rocha, *J. Am. Chem. Soc.*, 2003, **125**, 14573.

40 C. M, Kowalchuk, F. A. A. Paz, D. Ananias, P. Pattison, L. D. Carlos and J. Rocha, *Chem. Eur. J*, 2008, **14**, 8157.

41 S. Ferdov, R. A. S. Ferreira and Z. Lin, *Chem. Mater*, 2006, **18**, 5958.

42 C. Wickleder, I. Hartenbach, P. Lauxmann, T. Schleid, *Zeitschrift fuer Anorganische und Allgemeine Chemie*, 2002, **628**, 1602.

43 P.Y. Chiang, T.W. Lin, J.H. Dai, JH, B.C. Chang, K.H. Lii, *Inorg. Chem*, 2007, **46**, 3619.

44 R. C. Evans, D. Ananias, A. Douglas, P. Douglas, L. D. Carlos and J. Rocha, *J. Phys. Chem. C*, 2008, **112**, 260.

45 X. Wang, J. Li, G. Wang, Y. Han, T. Su, Y. Li, J. Y and R. Xu, *Solid State Sciences*, 2010, **12**, 422.

46 M. F. Tang, P. Y. Chian, Y. H. Su, Y. C. Jung, G. Y. Hou, B. C. Chang and K. H. Lii, *Inorg. Chem*, 2008, **47**, 8985.

47 X. J. Kang, S. S. Huang, P. P Yang, P. A. Ma, D. M. Yang and J. Lin, *Dalton Trans*, 2011, **40**, 1873.

48 D. L. Geng, G.G. Li, M. M. Shang, C. Peng, Y. Zhang, Z.Y. Cheng and J. Lin, *Dalton Trans*, 2012, **41**, 3078.

49 Z. L. Fu, X. J. Wang, Y. M. Yang, Z. J. Wu, D. F. Duan and X. H. Fu, *Dalton Trans*, 2014, **43**, 2819.

50 P. L. Chen, P. Y. Chiang, H. C. Yeh, B. C. Chang and K. H. Lii, *Dalton Trans*, 2008, 1721.